

## Original Article

# <sup>18</sup>F-Fluorodeoxyglucose positron emission tomography/computed tomography in patients with Kikuchi-Fujimoto disease: a nine-case series in China

Jun Zhang<sup>1\*</sup>, Meng-Jie Dong<sup>1\*</sup>, Kan-Feng Liu<sup>2</sup>, Li-Ming Xu<sup>3</sup>, Kui Zhao<sup>2</sup>, Jun Yang<sup>1</sup>, Wan-Wen Weng<sup>1</sup>, Hong Qiu<sup>4</sup>, Li-Li Lin<sup>2</sup>, Yang-Jun Zhu<sup>1</sup>

<sup>1</sup>Department of Nuclear Medicine, The First Affiliated Hospital, College of Medicine, Zhejiang University, Hangzhou, China; <sup>2</sup>Positron Emission Tomography Center, The First Affiliated Hospital, College of Medicine, Zhejiang University, Hangzhou, China; <sup>3</sup>Department of Pathology, The First Affiliated Hospital, College of Medicine, Zhejiang University, Hangzhou, China; <sup>4</sup>General Intensive Care Unit, The First Affiliated Hospital, College of Medicine, Zhejiang University, Hangzhou, China. \*Equal contributors.

Received August 24, 2015; Accepted October 25, 2015; Epub November 15, 2015; Published November 30, 2015

**Abstract:** This study observed the image characteristics and clinico-imaging relationships of <sup>18</sup>F-fluorodeoxyglucose positron emission tomography/computed tomography (<sup>18</sup>F-FDG PET/CT) in the patients with Kikuchi-Fujimoto disease (KFD). Nine consecutive patients with histologically proven KFD who underwent <sup>18</sup>F-FDG PET/CT were recruited. The <sup>18</sup>F-FDG uptakes of bone marrow (BM), spleen and lymph nodes (LNs) were systematically evaluated and maximum standardized uptake values (SUVmax) were measured. The number, locations and size factors of LNs were also assessed. The correlations were calculated between <sup>18</sup>F-FDG uptake and laboratory data and size factors of LNs, and the findings of LNs were compared between subgroups with different clinical features. <sup>18</sup>F-FDG uptakes were positive in the BM (SUVmax,  $3.2 \pm 1.2$ ), spleen (SUVmax,  $2.8 \pm 0.7$ ) and 122 affected LNs (SUVmax,  $4.2 \pm 2.2$ ) for all patients. The affected LNs presented a systemically (region,  $4 \pm 1$ ), multiple (number,  $14 \pm 5$ ) and small-sized (long axis diameter,  $11.4 \pm 2.7$  mm; short axis diameter,  $8.0 \pm 2.1$  mm; area,  $81.1 \pm 44.6$  mm<sup>2</sup>) pattern. The SUVmax of BM correlated to neutrophil count, and the SUVmax of affected LNs correlated to size factors and was lower in patients with long imaging interval and positive anti-nuclear antibody (ANA) ( $P < 0.05$ ). We conclude that <sup>18</sup>F-FDG PET/CT can be characterized by the generalized distribution of relatively small-sized LNs and involvement of BM and spleen with high <sup>18</sup>F-FDG avidity in patients with KFD. The imaging interval, neutrophil count and ANA level should be synthetically considered during imaging evaluation.

**Keywords:** Kikuchi-Fujimoto disease, lymphadenopathy, <sup>18</sup>F-fluorodeoxyglucose, positron emission tomography/computed tomography

## Introduction

Kikuchi-Fujimoto disease (KFD) is firstly described independently in 1972 by Kikuchi [1] and Fujimoto et al [2], usually characterized by fever and histiocytic necrotizing lymphadenitis, mostly involving cervical nodes. Clinically, KFD can resemble lymphoma, tuberculosis, and systemic lupus erythematosus (SLE) and it is difficult to accurately diagnose KFD based on physical findings or imaging alone. After excisional lymph node biopsy, the diagnosis is made histologically by identifying eccentric, crescent-shaped nuclei of histiocytes, karyor-

rhectic debris, and plasmacytoid monocytes in the form of nodules, with a paucity of neutrophils [3].

<sup>18</sup>F-fluorodeoxyglucose positron emission tomography/computed tomography (<sup>18</sup>F-FDG PET/CT) has come to be recognized as a useful imaging technique for the detection and diagnosis of inflammatory conditions, including fever of unknown origin [4], inflammatory bowel disease [5], and adult-onset Still's disease [6]. In recent years, a few case reports of <sup>18</sup>F-FDG PET/CT findings have suggested that a high <sup>18</sup>F-FDG uptake was exhibited in affected lymph

# 18F-FDG PET/CT in Kikuchi-Fujimoto disease

**Table 1.** Characteristics of patients, laboratory data and follow-up

	1	2	3	4	5	6	7	8	9
Age (years)/Sex	17/F	18/M	38/F	57/F	33/M	48/F	60/F	19/M	42/M
Disease duration (days)	51	63	22	32	135	61	26	26	114
Imaging interval (days)	42	51	14	40	21	126	8	20	108
Clinical features									
Fever (Celsius)	+(40.0)	+(39.4)	+(40.2)	+(39.5)	+(40.0)	+(39.8)	+(40.2)	+(40.3)	+(40.0)
Sore throat	+	+	-	-	-	-	+	-	-
Skin rash	-	-	-	+	-	+	-	+	-
Weight loss (Kg)	+(5)	-	-	-	-	-	+(5)	-	-
Myalgia	-	-	-	-	-	-	+	+	-
Arthralgia	-	-	-	+	-	-	-	-	-
Cervical lymphadenopathy	+	-	+	-	+	-	+	+	+
Laboratory data									
Hemoglobin (131-172g/l)	120	152	118	110	148	109	98	128	121
Leukocyte (4-10×10 <sup>9</sup> /l)	4.8	4.5	2.3	5.2	3.5	4.3	1.6	1.1	1.2
Neutrophil (2-7×10 <sup>9</sup> /l)	2.2	3.0	1.4	3.9	2.1	2.8	1.0	0.5	0.8
Platelet (83-303×10 <sup>9</sup> /l)	208	111	178	104	97	118	61	145	123
ALT (5-35 U/l)	55	389	20	309	38	489	167	53	81
AST (8-40 U/l)	18	143	33	423	31	725	613	72	141
LDH (109-245 U/l)	ND	ND	522	1376	381	830	885	ND	313
CRP (0-8 mg/dl)	14.2	3.1	16.9	41.8	22.5	16.4	22.4	20.1	8.6
ESR (0-20 mm/h)	73	4	49	14	59	9	70	30	44
SF (7-323 ng/ml)	236	ND	466	>40000	638	5929	503	1163	402
ANA	-	-	-	-	-	-	+ 1:80	+ 1:80	+ 1:160
Bone marrow biopsy	AP	AP	AP	AP	WP	AP	AP	WP	AP
Response to AB/GC	-/+	-/+	-/+	-/+	-/NA	-/+	-/+	-/+	-/+
Follow-up (Celsius)	R	R	R(37.2)	R(37.4)	R(37.0)	R(36.9)	R(37.1)	R	R(36.6)

F, female; M, male; ALT, alamine aminotransferase; AST, aspartate aminotransferase; LDH, lactate dehydrogenase; CRP, C-reactive protein; ESR, erythrocyte sedimentation rate; SF, serum ferritin; ANA, anti-nuclear antibody; AB, antibiotics; GC, glucocorticoids; +, positive; -, negative; ND, not done; AP, active proliferation; WP, weak proliferation; NA, not administrated; R, remission.

nodes (LNs) of patients with KFD [7-11]. Furthermore, several studies based on small sample sizes have evaluated the imaging features and diagnosis usefulness of <sup>18</sup>F-FDG PET/CT in Japanese [12, 13] and Korean [14, 15] patients with KFD. Herein, we wished to observe the image characteristics and clinico-imaging relationships of <sup>18</sup>F-FDG PET/CT in Chinese patients with KFD.

## Materials and methods

### Patient

This study was reviewed and approved by ethics committee of our hospital. Due to the purely retrospective and observational nature of the study, informed consent was waived. A total of 33 consecutive patients with histologically

proven KFD by lymph node excision biopsy were reviewed retrospectively at our hospital between January 2007 and December 2014. Among them, nine patients who underwent <sup>18</sup>F-FDG PET/CT without any immunosuppressive treatment before PET/CT scan were finally recruited in this study. All patients had no history of chronic infection or autoimmune disease. The laboratory data were obtained within 2 weeks before PET/CT. All patients underwent ultrasonography and unenhanced CT before PET/CT, and bone marrow examination and further clinical follow-up, ruling out lymphoma and similar disorders.

### PET/CT techniques

Patients were instructed to avoid strenuous work or exercise for ≥24 h and to fast >4 h and

# 18F-FDG PET/CT in Kikuchi-Fujimoto disease

**Table 2.** Imaging characteristics of <sup>18</sup>F-FDG PET/CT

Case	Liver (SUVmax)	Spleen (SUVmax)	BM (SU- Vmax)	Affected LN with positive uptake					Other positive le- sions (SUVmax)
				SUVmax	Number and location	Size factor (range)			
						LAD (mm)	SAD (mm)	Area (mm <sup>2</sup> )	
1	1.4	1.6 +	2.2 +	2.2-8.7 +	7, cervical (BL); 3, axillary (BL); 1, mediastinal; 1, abdominal	6.3-17.8	5.8-11.7	23.0-198.0	
2	2.1	2.6 +	2.6 +	2.8-7.2 +	2, cervical (BL); 2, abdominal	6.3-14.4	6.0-13.9	40.0-140.0	
3	2.4	3.4 +	3.2 +	3.0-12.8 +	6, cervical (BL); 3, axillary (BL); 7, mediastinal; 1, pelvic (UL)	7.4-15.1	4.6-10.4	33.0-149.0	
4	1.9	3.4 +	5.6 +	2.0-12.1 +	1, cervical (UL); 1, mediastinal; 4, abdominal; 2, pelvic (UL); 1, inguinal (UL)	7.2-16.8	5.3-13.3	33.0-133.0	
5	1.9	3.6 +	3.1 +	2.7-7.4 +	1, cervical (UL); 3, axillary (BL); 7, abdominal, 2, pelvic (BL)	8.6-14.2	6.3-11.3	50.0-149.0	rectum (3.9)
6	2.4	3.7 +	4.7 +	2.5-5.2 +	3, cervical (BL), 5, axillary (BL), 2, abdominal, 4, pelvic (BL)	8.9-13.8	5.0-12.6	33.0-182.0	ascending colon (5.6)
7	1.6	2.1 +	2.2 +	1.8-6.0 +	4, cervical (BL); 2, axillary (BL); 2, abdominal; 2, pelvic (BL); 2, inguinal (BL)	9.2-16.9	5.9-14.0	50.0-280.0	
8	2.3	2.7 +	2.5 +	3.0-5.6 +	8, cervical (BL); 6, axillary (BL); 4, abdominal; 2, pelvic (BL)	7.6-20.2	5.2-12.1	50.0-176.0	
9	1.5	2.2 +	3.1 +	1.6-6.9 +	2, cervical (UL); 8, axillary (BL); 7, abdominal; 1, pelvic (UL); 3, inguinal (BL)	5.8-14.9	4.5-11.8	17.0-149.0	gastric mucosa (2.2)

<sup>18</sup>F-FDG PET/CT, <sup>18</sup>F-fluorodeoxyglucose positron emission tomography/computed tomography; SUVmax, maximum standard uptake value; BM, bone marrow; LN, lymph node; LAD, long axis diameter; SAD, short axis diameter; BL, bilateral; UL, unilateral; +, positive.

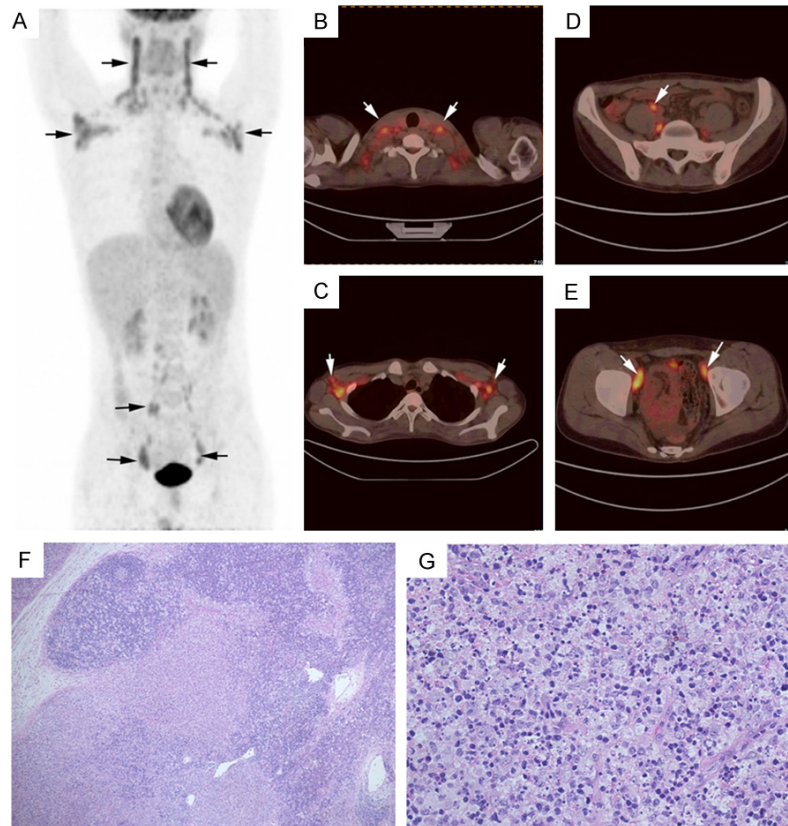


**Figure 1.** A 19-year-old male patient with Kikuchi-Fujimoto disease (case 8). (A) Maximum intensity projection image of  $^{18}\text{F}$ -fluorodeoxyglucose positron emission tomography/computed tomography ( $^{18}\text{F}$ -FDG PET/CT) shows intense accumulation of  $^{18}\text{F}$ -FDG in bilateral cervical including supraclavicular, bilateral axillary, abdominal and pelvic area (black arrows); (B, E) Axial images show the affected lymph nodes with increased  $^{18}\text{F}$ -FDG uptake in cervix, axilla, abdomen, and pelvis, respectively (white arrows); (F, G) Histological images of hypermetabolic lymph node in left cervix show the disrupt structure of lymph node with plenty of lymphohistiocytic cells, karyorrhectic nuclear debris, and extensive necrosis, and without polymorphonuclear leukocytes. (H&E; F  $\times 50$ ; G  $\times 400$ ).

had a pre-scan blood glucose measurement to ensure a level  $<200$  mg/dl before intravenous injection of  $^{18}\text{F}$ -FDG at 5.5-7.4 MBq/kg body-weight. One hour after injection, PET/CT images were acquired from the vertex to the upper thighs. Studies were performed using combined PET/CT (Siemens Biograph 16 HR). Unenhanced CT for attenuation correction and anatomical localization was acquired before PET with 100 mA/s at 120 kV. All CT images were reconstructed with a slice thickness of 5 mm. After CT, PET was acquired for 16.2 cm per bed position. Reconstructed PET images, CT images, and fused images of matching pairs of PET and CT images were available for review in axial, coronal, and sagittal planes, as well as in maximum-intensity projections and three-dimensional cine mode.

axis diameter, LAD; short axis diameter, SAD; and area) were evaluated systematically.

#### Statistical analysis

Continuous values are summarized as means  $\pm$  standard deviation. Categorical variables are described in numbers and percentages. The calculation of correlations was evaluated using the Pearson correlation coefficient between  $^{18}\text{F}$ -FDG uptake and laboratory data and size factors of affected LNs. Nine patients were divided into two subgroups based on different clinical features, e.g. imaging interval (the duration between disease onset and PET/CT examination, which of more than 30 days was considered as long interval). Comparison between subgroups was made with independent-sam-

#### Data analysis

The intensity of  $^{18}\text{F}$ -FDG uptake on the PET/CT images at characteristic sites, such as the LNs, bone marrow (BM), spleen and liver, was evaluated and in consensus by two experienced nuclear medicine physicians. Regions of interest were drawn around each lesion and maximum standardized uptake values (SUVmax) were calculated.  $^{18}\text{F}$ -FDG uptake into these lesions was evaluated visually using the following scoring system [16]: 0, no uptake (same as bone); 1, slight uptake; 2, moderate uptake (same as the liver); 3, higher uptake than the liver and 4, highest uptake (SUVmax  $>4$ ). Each site with an  $^{18}\text{F}$ -FDG uptake score  $\geq 2$  was considered to show positive PET/CT findings. With regard to the affected LNs with positive uptake, the number, locations (categorized into six regions (unilateral or bilateral): cervical, axillary, mediastinal, abdominal, pelvic and inguinal region) and size factors (including long

**Table 3.** Correlations between  $^{18}\text{F}$ -FDG uptake and laboratory data

	Bone marrow		Spleen	
	<i>r</i>	<i>P</i>	<i>r</i>	<i>P</i>
Hemoglobin	-0.304	0.426	0.108	0.781
Leukocyte	0.474	0.197	0.260	0.499
Neutrophil	0.673	0.047*	0.397	0.290
Platelet	-0.210	0.588	-0.239	0.535
ALT	0.555	0.121	0.330	0.386
AST	0.496	0.174	0.226	0.558
CRP	0.621	0.074	0.421	0.259
ESR	-0.590	0.095	-0.491	0.180
SF	0.396	0.292	0.430	0.248

$^{18}\text{F}$ -FDG,  $^{18}\text{F}$ -fluorodeoxyglucose; ALT, alanine aminotransferase; AST, aspartate aminotransferase; LDH, lactate dehydrogenase; CRP, C-reactive protein; ESR, erythrocyte sedimentation rate; SF, serum ferritin; \*,  $P < 0.05$ .

ples T test. A probability value of less than 0.05 was considered to indicate significant difference. All statistical analyses were performed using the IBM SPSS statistics 19.0 (SPSS Inc., Chicago, IL, USA).

## Results

### Patient characteristics

**Table 1** showed the patient characteristics. There were three males and six female patients, with a mean age of  $36.9 \pm 16.5$  years. All patients suffered high fever, and six patients (66.7%) had cervical lymphadenopathy. The mean (range) of hemoglobin, leukocyte count, neutrophil count, platelet count, alanine aminotransferase (ALT), aspartate aminotransferase (AST), C-reactive protein (CRP), erythrocyte sedimentation rate (ESR), lactate dehydrogenase (LDH), and serum ferritin (SF) was  $122.7 \pm 17.7$  (98-152) g/l,  $3.2 \pm 1.6$  ( $1.1$ - $5.2$ )  $\times 10^9$ /l,  $2.0 \pm 1.1$  ( $0.5$ - $3.9$ )  $\times 10^9$ /l,  $127.2 \pm 44.2$  (61-208)  $\times 10^9$ /l,  $177.9 \pm 174.4$  (20-489) U/l,  $244.3 \pm 271.8$  (18-725) U/l,  $18.4 \pm 10.8$  (3.1-41.8) mg/dl,  $39.1 \pm 26.2$  (4-73) mm/h,  $717.8 \pm 397.3$  (313-1376) U/l, and  $6167.0 \pm 13801.4$  (236-40000) ng/ml, respectively. In addition, three patients were positive antinuclear antibody (ANA). Because of displaying the general distribution of  $^{18}\text{F}$ -FDG accumulation, PET/CT aided decisions regarding appropriate LNs biopsy sites in all patients. Upon being diagnosed as KFD, they were canceled the antibiot-

ics treatment without improvement, and then glucocorticoids were used in 8 patients with good response. At follow-up, all they recovered from lymphadenopathy and fever during  $58.9 \pm 40.6$  days.

### Quantitative PET/CT evaluation

**Table 2** showed the imaging characteristics of  $^{18}\text{F}$ -FDG PET/CT.  $^{18}\text{F}$ -FDG accumulation was positive in the BM, spleen and LNs for all patients. Homogeneously increased uptake of  $^{18}\text{F}$ -FDG was seen in the BM (mean of SUVmax,  $3.2 \pm 1.2$ ; range of SUVmax, 2.2-5.6) and spleen (mean of SUVmax,  $2.8 \pm 0.7$ ; range of SUVmax, 1.6-3.7). A total of 122 affected LNs were identified with positive uptake of  $^{18}\text{F}$ -FDG (mean of SUVmax,  $4.2 \pm 2.2$ ; range of SUVmax, 1.6-12.8). The affected LNs presented a systemically (mean of region,  $4 \pm 1$ ) and multiple (mean of number,  $14 \pm 5$ ) pattern. The cervix (27.9%, 34/122; bilateral in 6 patients, unilateral in 3 patients), axilla (24.6%, 30/122; bilateral in 7 patients) and abdomen (23.8%, 29/122; in 7 patients) were mainly involved regions. All affected LNs were almost oval and unfused with small size determined by CT (mean of LAD, SAD, and area:  $11.4 \pm 2.7$  mm,  $8.0 \pm 2.1$  mm, and  $81.1 \pm 44.6$  mm<sup>2</sup>, respectively). The 83.6% (102/122) of LNs were not more than 10 mm in SAD. In addition, the abnormal striped uptakes of rectum (SUVmax, 3.9; case 5), ascending colon (SUVmax, 5.6; case 6) and gastric mucosa (SUVmax, 2.2; case 9) were found in one patient respectively. **Figure 1** shows the  $^{18}\text{F}$ -FDG PET/CT appearance of a representative patient (case 8).

### Relationship between PET/CT measurement and laboratory data

Though SUVmax of BM correlated to count of neutrophil ( $P < 0.05$ ), no significant correlation was found between SUVmax (BM, spleen) and other laboratory data (counts of leukocyte and platelet or levels of hemoglobin, ALT, AST, CRP, ESR, and SF) (**Table 3**). For affected LNs, the means of SUVmax in patients with long imaging interval and ANA-positive were lower and the mean of area in patients with ANA-positive was bigger ( $P < 0.05$ ). However, the means of size factors and SUVmax of affected LNs were not statistically different between subgroups of normal and increased ESR or normal leukocyte and leukopenia (**Table 4**). In addition, the



**Table 4.** Comparison of affected LN findings in  $^{18}\text{F}$ -FDG PET/CT

Clinical subgroups		Number of patient, LN	Affected LN findings (mean $\pm$ standard deviation)			
			LAD	SAD	Area	SUVmax
Long interval ( >30 days)	No	4, 62	11.8 $\pm$ 2.6	8.1 $\pm$ 2.0	87.8 $\pm$ 45.7	4.90 $\pm$ 2.17
	Yes	5, 60	11.0 $\pm$ 2.8	8.0 $\pm$ 2.2	74.1 $\pm$ 42.7	3.56 $\pm$ 2.03
	<i>P</i>		0.146	0.745	0.090	0.001*
Leukopenia	No	4, 39	11.2 $\pm$ 3.1	8.1 $\pm$ 2.3	74.0 $\pm$ 47.4	4.02 $\pm$ 2.26
	Yes	5, 83	11.5 $\pm$ 2.6	8.0 $\pm$ 2.0	84.4 $\pm$ 43.1	4.34 $\pm$ 2.18
	<i>P</i>		0.522	0.897	0.235	0.452
Increased ESR	No	3, 27	10.8 $\pm$ 2.4	7.8 $\pm$ 2.4	71.3 $\pm$ 41.9	3.80 $\pm$ 2.35
	Yes	6, 95	11.6 $\pm$ 2.8	8.0 $\pm$ 2.0	83.8 $\pm$ 45.1	4.36 $\pm$ 2.15
	<i>P</i>		0.175	0.607	0.196	0.241
ANA-positive	No	6, 69	11.1 $\pm$ 2.6	7.9 $\pm$ 2.1	73.4 $\pm$ 41.4	4.86 $\pm$ 2.55
	Yes	3, 53	11.8 $\pm$ 2.9	8.2 $\pm$ 2.1	91.1 $\pm$ 46.9	3.43 $\pm$ 1.25
	<i>P</i>		0.175	0.349	0.029*	0.000*

LN, lymph node;  $^{18}\text{F}$ -FDG PET/CT,  $^{18}\text{F}$ -fluorodeoxyglucose positron emission tomography/computed tomography; LAD, long axis diameter; SAD, short axis diameter; SUVmax, maximum standard uptake value; ESR, erythrocyte sedimentation rate; ANA, antinuclear antibody; \*,  $P < 0.05$ .

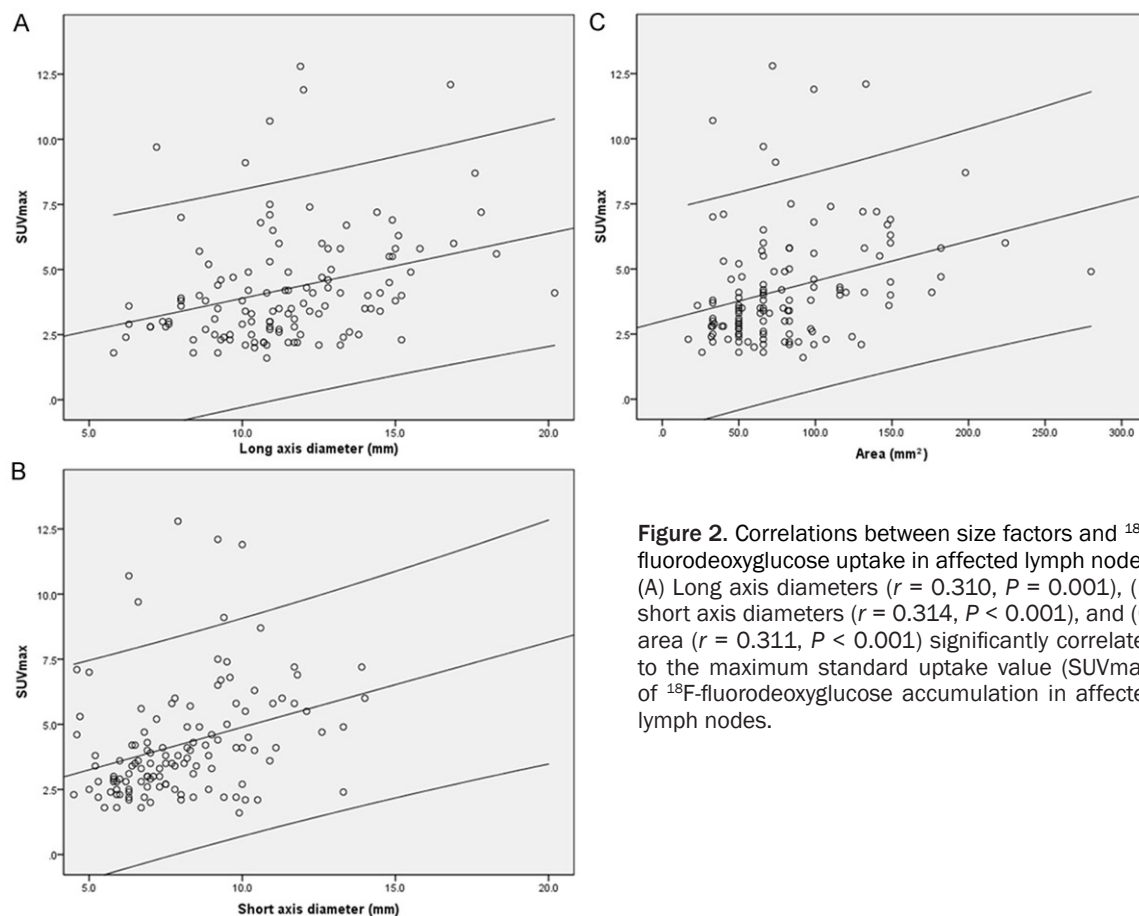


**Figure 2.** Correlations between size factors and  $^{18}\text{F}$ -fluorodeoxyglucose uptake in affected lymph nodes. (A) Long axis diameters ( $r = 0.310$ ,  $P = 0.001$ ), (B) short axis diameters ( $r = 0.314$ ,  $P < 0.001$ ), and (C) area ( $r = 0.311$ ,  $P < 0.001$ ) significantly correlated to the maximum standard uptake value (SUVmax) of  $^{18}\text{F}$ -fluorodeoxyglucose accumulation in affected lymph nodes.

SUVmax of affected LNs significantly correlated to LAD ( $r = 0.310$ ,  $P = 0.001$ ), SAD ( $r = 0.314$ ,  $P$

$< 0.001$ ), and area ( $r = 0.311$ ,  $P < 0.001$ ) (Figure 2).

## Discussion

KFD is considered an extremely rare, benign and self-limited disease, known as subacute necrotizing histiocytic lymphadenitis [13]. It has a worldwide distribution with higher prevalence among Asian, and usually happens to occur in young adults below 40 with a fourfold female predominance [17]. In the present study, nine consecutive KFD patients (mean age,  $36.9 \pm 16.5$  years) were recruited and female to male ratio was 2:1. Although the exact etiology of KFD is still unknown, it may be associated with CMV, EBV infection, or SLE and other autoimmune diseases [17, 18]. Our three patients were ANA-positive that may suggest the potential relationship between KFD and autoimmune diseases. Similar to previous results [17-23], fever (100%) and cervical lymphadenopathy (66.7%) were the main clinical manifestations, and throat sore, weight loss, myalgia, arthralgia, leucopenia, anemia, liver dysfunction, and elevated ESR, CRP, LDH, and SF were also observed in our study. It may indicate seriously clinical conditions for our cases, because elevation of ESR, ALT, AST, and LDH, especially LDH, may relate to the severity of the disease [24].

Up to now, it remains difficult to accurately diagnosing KFD because of its very low incidence, non-specifically clinical manifestations, laboratory tests and radiologic findings. And so, KFD is frequently misdiagnosed as malignant lymphoma or some other form of inflammatory disease [10, 17, 18].  $^{18}\text{F}$ -FDG PET/CT is a noninvasive metabolic imaging that plays an important role in the management of oncology patients. It is well recognized that  $^{18}\text{F}$ -FDG is taken not only in malignant cells but also in macrophages and other activated inflammatory cells at the site of inflammation or infection [4-6]. Since PET imaging of KFD was first reported by Liao et al in 2003 [7], some case reports [8-11] have depicted the basically common characteristics of  $^{18}\text{F}$ -FDG uptake, namely high avidity of  $^{18}\text{F}$ -FDG mimicking malignant lymphoma in affected LNs of KFD patients. Subsequently, Ito K et al [12] and Kong E et al [14] retrospectively analyzed the features of  $^{18}\text{F}$ -FDG uptake of LNs on 7 Japanese and 22 Korean patients with KFD, respectively. They showed that KFD could present multiply gener-

alized distribution of the relatively small-sized hypermetabolic LNs in body on  $^{18}\text{F}$ -FDG PET/CT.

We describe firstly here the  $^{18}\text{F}$ -FDG PET/CT imaging in 9 Chinese patients with KFD. Our study confirmed that  $^{18}\text{F}$ -FDG PET/CT could be used to visualize the degree and extent of KFD by providing whole-body metabolic values and morphologic abnormalities. In our cases,  $^{18}\text{F}$ -FDG PET/CT revealed mainly accumulation in the multiple LNs (SUVmax,  $4.2 \pm 2.2$ ). Intense  $^{18}\text{F}$ -FDG uptake in affected LNs of KFD may be associated with high phagocytic activity of proliferated histiocytes. Necrotic foci themselves should not show high  $^{18}\text{F}$ -FDG uptake, but necrotizing lymphocytes and numerous histiocytes surrounding the necrotic foci are anticipated to have high  $^{18}\text{F}$ -FDG accumulation on KFD patients [14]. BM and spleen involvements were also observed with homogenous uptake of  $^{18}\text{F}$ -FDG (SUVmax,  $3.2 \pm 1.2$  and  $2.8 \pm 0.7$ , respectively) in the present study. Abnormal accumulation of  $^{18}\text{F}$ -FDG in BM may be owing to enhanced metabolism of BM for increasing leukocyte production when inflammation occur [6].  $^{18}\text{F}$ -FDG uptake in BM was correlated specifically with the neutrophil count, suggesting that  $^{18}\text{F}$ -FDG uptake by BM reflects metabolism in BM that is regulated mainly by granulocyte progenitors and stimulated by endogenous hematopoietic growth factors [25]. Similarly, our result also indicated the significant correlation between  $^{18}\text{F}$ -FDG uptake of BM and neutrophil count in patients with KFD. For diffuse uptake of  $^{18}\text{F}$ -FDG in spleen, it can be associated with inflammation involvement of KFD. In the patients with diffuse splenic  $^{18}\text{F}$ -FDG uptake, the CRP level and leukocyte count were significantly higher [26]. To date, the gastroenteric involvement is unreported in patients with KFD, while we found the abnormal striped uptakes of rectum, ascending colon and gastric mucosa in one patient respectively. We surmise that it may be the gastroenteritis leading to high accumulation of  $^{18}\text{F}$ -FDG in digestive tract, even if endoscope was not done to confirm it.

However,  $^{18}\text{F}$ -FDG accumulation in the multiple LNs, BM, and spleen may be not specific for the patients with KFD. Some systemically inflammatory processes and hematologic malignancies may also show similar imaging characteristics. Oh et al [27] revealed that  $^{18}\text{F}$ -FDG PET/CT

could successfully visualize hyperactive LNs in 18 patients (56%), BM in 15 patients (47%) and spleen in 13 patients (41%) with systemic autoimmune disease. Additionally, the BM and spleen are common sites involved in lymphoma, and the incidences have been reported to be 5~80% and 20~40 %, respectively [28]. In recent years, Tsujikawa et al [13] reported that KFD could be distinguished from non-Hodgkin lymphoma using SUV and partial volume corrected SUV of affected LNs on eight KFD patients. Nevertheless, Kim et al [15] found that there were no significant differences in SUVmax of affected LNs between KFD and malignant lymphoma. It is worth exploring whether there was a statistical difference of <sup>18</sup>F-FDG uptake between KFD and other disease such as infection, non-specific inflammation or lymphoma based on a large sample size in the future.

Formerly, KFD usually is considered rarely involving extra-cervical regions, such as mediastinal, peritoneal or retroperitoneal regions of the body, and only 1%-22% patients undergo generalized lymphadenopathy [18]. But recent PET/CT studies displayed that almost all patients with KFD were multiply generalized distribution of affected LNs, including cervical and extra-cervical lesions [12, 14]. The size of affected LNs is commonly smaller than 4 cm [17]. Kong E et al reported that 71% LNs were less than 1 cm in their SAD determined by CT [14]. Likewise, our analysis found that the cervical region was the most common location with about 28% affected LNs in all patients, while extra-cervical involvements also were not rare with approximate a quarter of affected LNs of axillary and abdominal regions in 7 patients. In addition, all affected LNs were almost oval and unfused with small sizes, and the SAD was less than 1 cm in 83.6% affected LNs in our patients.

We confirmed that sizes factors (LAD, SAD and area) of affected LNs were significantly correlated with the SUVmax, suggesting the SUVmax is influenced by lesion size in general. These findings are not identical to the results reported by Ito K et al [12]. They stated that there was no significant correlation between size factors (the maximum diameter and the areas) of affected LNs and <sup>18</sup>F-FDG accumulations. This discrepancy can be attributed to the different sizes of the datasets. Furthermore, we compared the <sup>18</sup>F-FDG PET/CT findings of affected LNs

between patients with differently clinical features. The results showed that the patients with long imaging interval had significantly lower SUVmax. This may be attributed the feature of KFD with recovering spontaneously during 1 to 4 months [17]. The longer interval implies lower <sup>18</sup>F-FDG avidity in gradually recovered LNs. We also noted that the ANA-positive patients had bigger sizes and lower <sup>18</sup>F-FDG uptake of LNs. At necrotic sites in the LNs of KFD, abundant apoptotic cells express autoantigens. Impaired ability to clear these cells and inappropriate activation of CD8 T cells are associated with the producing of autoantibodies and development of some autoimmune diseases [29]. We consider that the inflammatory reaction resulting from ANA and its immunocomplex with autoantigen may be contribute to the larger size of LNs in ANA-positive patients with KFD. As for lower FDG uptake of LNs in ANA-positive patients, it may suggest a relatively fewer amount or weaker phagocytic activity of histiocytes in these patients. Of course, the speculation need to be histopathologically demonstrated by further research.

In contrast to conventional imaging methods, <sup>18</sup>F-FDG PET/CT reflects glucose metabolism and enables estimation of the disease activity of lesions [6]. Hence, <sup>18</sup>F-FDG PET/CT can be a useful tool to localize an appropriate biopsy site, especially in cases with a negative result using conventional imaging methods. In our study, <sup>18</sup>F-FDG PET/CT aided decisions regarding appropriate biopsy sites of LNs, thereby ruling out lymphoma and similar disorders. And thus, the clinical managements of 8 patients were changed from the antibiotics treatment without improvement to glucocorticoids administration with good response.

At last, some limitations should be considered. First, our study was conducted at single institution and the patients' cohort was relatively small. Second, this study was retrospective. Third, the comparison was not done between KFD and malignant lymphoma. Hence, a prospective study of <sup>18</sup>F-FDG PET/CT in more patients with KFD is needed to contextualize our findings.

## Conclusion

In conclusion, our findings indicate that <sup>18</sup>F-FDG PET/CT is a unique imaging method for assess-



ment of metabolic activity throughout the body in those with KFD, which can be characterized by the generalized distribution of relatively small-sized LNs and involvement of BM and spleen with high  $^{18}\text{F}$ -FDG avidity. Furthermore, the synthetical consideration with imaging interval, neutrophil count and ANA level should be needed during imaging evaluation.

### Acknowledgements

The present work was supported by the National Natural Science Foundation of China (No. 81471704), the Science and Technology Planning Project of Zhejiang Province (2013C33119), and the Health Bureau Project of Zhejiang Province (2013KYA069, 2013KYB111, 2013ZDA008).

### Disclosure of conflict of interest

None.

**Address correspondence to:** Dr. Yang-Jun Zhu, Department of Nuclear Medicine, The First Affiliated Hospital, College of Medicine, Zhejiang University, 79 Qingchun Road, Hangzhou 310003, Zhejiang, China. Tel: 86-571-87236510; Fax: 86-571-87236519; E-mail: hz\_zyj@126.com

### References

- [1] Kikuchi M. Lymphadenitis showing focal reticulum cell hyperplasia with nuclear debris and phagocytes: a clinicopathological study. *Acta Hematol Jpn* 1972; 35: 379-380.
- [2] Fujimoto Y, Kozima Y and Yamaguchi K. Cervical subacute necrotizing lymphadenitis: a new clinicopathologic entity. *Naika* 1972; 20: 920-927.
- [3] Lee BC and Patel R. Kikuchi-Fujimoto disease: a 15-year analysis at a children's hospital in the United States. *Clin Pediatr (Phila)* 2013; 52: 92-95.
- [4] Dong MJ, Zhao K, Liu ZF, Wang GL, Yang SY and Zhou GJ. A meta-analysis of the value of fluorodeoxyglucose-PET/PET-CT in the evaluation of fever of unknown origin. *Eur J Radiol* 2011; 80: 834-844.
- [5] Zhang J, Li LF, Zhu YJ, Qiu H, Xu Q, Yang J, Weng WW and Liu NH. Diagnostic performance of  $^{18}\text{F}$ -FDG-PET versus scintigraphy in patients with inflammatory bowel disease: a meta-analysis of prospective literature. *Nucl Med Commun* 2014; 35: 1233-1246.
- [6] Dong MJ, Wang CQ, Zhao K, Wang GL, Sun ML, Liu ZF and Xu L.  $^{18}\text{F}$ -FDG PET/CT in patients with adult-onset Still's disease. *Clin Rheumatol* 2015; 34: 2047-56.
- [7] Liao AC, Chen YK. Cervical lymphadenopathy caused by Kikuchi disease: positron emission tomographic appearance. *Clin Nucl Med* 2003; 28: 320-321.
- [8] Kim CH, Hyun OJ, Yoo IeR, Kim SH, Sohn HS and Chung SK. Kikuchi Disease Mimicking Malignant Lymphoma on FDG PET/CT. *Clin Nucl Med* 2007; 32: 711-712.
- [9] Kaicker S, Gerard PS, Kalburgi S, Geller MD and Hailoo D. PET-CT scan in a patient with Kikuchi disease. *Pediatr Radiol* 2008; 38: 596-597.
- [10] Ito K, Morooka M and Kubota K. F-18 FDG PET/CT findings showing lymph node uptake in patients with Kikuchi disease. *Clin Nucl Med* 2009; 34: 821-822.
- [11] Zhang MJ, Xiao L, Zhu YH, Jiang JJ, Jiang MS and He W. Lymph node uptake of  $^{18}\text{F}$ -fluorodeoxyglucose detected with positron emission tomography/computed tomography mimicking malignant lymphoma in a patient with Kikuchi disease. *Clin Lymphoma Myeloma Leuk* 2010; 10: 477-479.
- [12] Ito K, Morooka M and Kubota K. Kikuchi disease:  $^{18}\text{F}$ -FDG positron emission tomography/computed tomography of lymph node uptake. *Jpn J Radiol* 2010; 28: 15-19.
- [13] Tsujikawa T, Tsuchida T, Imamura Y, Kobayashi M, Asahi S, Shimizu K, Tsuji K, Okazawa H and Kimura H. Kikuchi-Fujimoto disease: PET/CT assessment of a rare cause of cervical lymphadenopathy. *Clin Nucl Med* 2011; 36: 661-664.
- [14] Kong E, Chun K, Hong Y, Hah J and Cho I.  $^{18}\text{F}$ -FDG PET/CT findings in patients with Kikuchi disease. *Nuklearmedizin* 2013; 52: 101-106.
- [15] Kim JE, Lee EK, Lee JM, Bae SH, Choi KH, Lee YH, Hah JO, Choi JH, Kong EJ and Cho IH. Kikuchi-Fujimoto disease mimicking malignant lymphoma with 2- $^{18}\text{F}$ fluoro-2-deoxy-D-glucose PET/CT in children. *Korean J Pediatr* 2014; 57: 226-231.
- [16] Kubota K, Ito K, Morooka M, Mitsumoto T, Kurihara K, Yamashita H, Takahashi Y and Mimori A. Whole-body FDG-PET/CT on rheumatoid arthritis of large joints. *Ann Nucl Med* 2009; 23: 783-791.
- [17] Bosch X, Guilabert A, Miquel R and Campo E. Enigmatic Kikuchi-Fujimoto disease: a comprehensive review. *Am J Clin Pathol* 2004; 122: 141-152.
- [18] Jamal AB. Kikuchi fujimoto disease. *Clin Med Insights Arthritis Musculoskelet Disord* 2012; 5: 63-66.

- [19] Kucukardali Y, Solmazgul E, Kunter E, Oncul O, Yildirim S and Kaplan M. Kikuchi-Fujimoto disease: analysis of 244 cases. *Clin Rheumatol* 2007; 26: 50-54.
- [20] Kim TY, Ha KS, Kim Y, Lee J, Lee K and Lee J. Characteristics of Kikuchi-Fujimoto disease in children compared with adults. *Eur J Pediatr* 2014; 173: 111-116.
- [21] Yu HL, Lee SS, Tsai HC, Huang CK, Chen YS, Lin HH, Wann SR, Liu YC and Tseng HH. Clinical manifestations of Kikuchi's disease in southern Taiwan. *J Microbiol Immunol Infect* 2005; 38: 35-40.
- [22] Nakamura I, Imamura A, Yanagisawa N, Suganuma A and Ajisawa A. Medical study of 69 cases diagnosed as Kikuchi's disease. *Kansenshogaku Zasshi* 2009; 83: 363-368.
- [23] Chuang CH, Yan DC, Chiu CH, Huang YC, Lin PY, Chen CJ, Yen MH, Kuo TT and Lin TY. Clinical and laboratory manifestations of Kikuchi's disease in children and differences between patients with and without prolonged fever. *Pediatr Infect Dis J* 2005; 24: 551-554.
- [24] Kikuchi M and Ohshima K. Cervical Lymphadenopathy, Fever and Leukopenia (Histiocytic-Necrotizing Lymphadenitis or Kikuchi Disease). *Pathology Case Reviews* 2004; 9: 199-205.
- [25] Murata Y, Kubota K, Yukihiro M, Ito K, Watanabe H and Shibuya H. Correlations between 18F-FDG uptake by bone marrow and hematological parameters: measurements by PET/CT. *Nucl Med Biol* 2006; 33: 999-1004.
- [26] Kim K, Kim SJ, Kim IJ, Kim DU, Kim H, Kim S and Ahn SH. Factors associated with diffusely increased splenic F-18 FDG uptake in patients with cholangiocarcinoma. *Nucl Med Mol Imaging* 2014; 48: 137-143.
- [27] Cremers JP, Van Kroonenburgh MJ, Mostard RL, Vöo SA, Wijnen PA, Koek GH and Drent M. Extent of disease activity assessed by 18F-FDG PET/CT in a Dutch sarcoidosis population. *Sarcoidosis Vasc Diffuse Lung Dis* 2014; 31: 37-45.
- [28] Oh JR, Song HC, Kang SR, Yoo SW, Kim J, Chong A, Min JJ, Bom HS, Lee SS and Park YW. The clinical usefulness of (18) F-FDG PET/CT in patients with systemic autoimmune disease. *Nucl Med Mol Imaging* 2011; 45: 177-184.
- [29] Ogata S, Bando Y, Saito N, Katsuoka K and Ishii M. Kikuchi-Fujimoto disease developed into autoimmune disease: a report of two cases. *Mod Rheumatol* 2010; 20: 301-305.